The nuclear envelope lamina network has elasticity and a compressibility limit suggestive of a molecular shock absorber

Kris Noel Dahl[1], Samuel M. Kahn[1], Katherine L. Wilson[2] and Dennis E. Discher[1,*]

[1]Department of Chemical and Biomolecular Engineering, 220 South 33rd Street, University of Pennsylvania, Philadelphia, PA 19104-6393, USA
[2]Department of Cell Biology, Johns Hopkins University, 3400 North Wolfe Street, Baltimore, MD 21205-2105, USA
*Author for correspondence (e-mail: discher@seas.upenn.edu)

Accepted 14 June 2004
Journal of Cell Science 117, 4779-4786 Published by The Company of Biologists 2004
doi:10.1242/jcs.01357

Summary

Mechanical properties of the nuclear envelope have implications for cell and nuclear architecture as well as gene regulation. Using isolated *Xenopus* oocyte nuclei, we have established swelling conditions that separate the intact nuclear envelope (membranes, pore complexes and underlying lamin filament network) from nucleoplasm and the majority of chromatin. Swelling proves reversible with addition of high molecular mass dextrans. Micropipette aspiration of swollen and unswollen nuclear envelopes is also reversible and yields a network elastic modulus, unaffected by nucleoplasm, that averages 25 mN/m. Compared to plasma membranes of cells, the nuclear envelope is much stiffer and more resilient. Our results suggest that the nuclear lamina forms a compressed network shell of interconnected rods that is extensible but limited in compressibility from the native state, thus acting as a 'molecular shock absorber'. In light of the conservation of B-type lamins in metazoan evolution, the mechanical properties determined in this investigation suggest physical mechanisms by which mutated lamins can either destabilize nuclear architecture or influence nuclear responses to mechanical signals in Emery-Dreifuss muscular dystrophy, cardiomyopathy, progeria syndromes (premature 'aging') and other laminopathies.

Key words: Nuclear envelope, Nuclear lamina, Membranes, Biomechanics/elasticity, Cell nucleus structures

Introduction

Cells respond to mechanical cues from their environment in part through changes in gene expression. Compression-induced changes in the shapes of chondrocyte nuclei, for example, correlate with changes in cartilage composition and density (Guilak, 1995). Endothelial cells likewise modify gene expression in response to shear stress (Papadaki and Eskin, 1997). In endothelial cells, physical force is transmitted via a pathway from integrins to the cytoskeleton to the nuclear envelope and nuclear interior (Maniotis et al., 1997). The nature of this proposed mechanical coupling, particularly across the nuclear envelope, is not yet understood. Models suggest 'bridging' interactions by conserved spectrin-repeat- or Sun-domain-containing proteins situated in both membranes of the nuclear envelope (Lee et al., 2002; Zhang et al., 2002; Zhen et al., 2002). In somatic cells, most nuclear inner membrane proteins are anchored to lamins, which form stable filament networks near the inner nuclear membrane and in the nuclear interior (Gruenbaum et al., 2003). The nuclear envelope also has physical connections to chromatin via lamins, which bind directly to chromatin (Moir et al., 1995) and to chromatin-binding nuclear membrane proteins (Burke and Stewart, 2002; Gant and Wilson, 1997). Although the exact mechanisms governing force transduction are unknown, nuclear envelope stiffness is a hypothesized regulator of the effects of cellular forces on chromatin or gene expression.

Although the typical cell nucleus is spheroidal, some differentiated cells undergo dramatic but regulated changes in nuclear morphology. Examples include multi-lobed nuclei in neutrophils (Yabuki et al., 1999) and elongated nuclei in spermatids (Dadoune, 2003). Aberrations in nuclear morphology, more than cell morphology, also identify cancerous tissue (Bissell et al., 1999). At least eight diseases have been linked to mutations in A-type lamins or lamin-binding proteins of the nuclear inner membrane. These diseases include Emery-Dreifuss muscular dystrophy, dilated cardiomyopathy with conduction system disease (Burke and Stewart, 2002), and Hutchinson-Gilford progeria syndrome, a devastating 'premature aging' syndrome (De Sandre-Giovannoli et al., 2003; Eriksson et al., 2003). Heterozygous mutations in laminin B receptor (LBR), a membrane protein that binds lamin B, cause the dominant Helger-Puet anomaly of white blood cell nuclear shape; homozygous defects in LBR are linked to bone and cartilage disorders and developmental delay (Hoffmann et al., 2002). Proposed disease mechanisms include defects in tissue-specific gene expression coupled to mechanical weakness of the nuclear envelope (Morris, 2001; Wilson, 2000; Zastrow et al., 2004).

The *Xenopus* oocyte (XO) nucleus has a diameter about twenty times larger than typical somatic nuclei, but its chromatin content is similar. Thus the mechanical properties of

the XO nuclear envelope are less influenced by chromatin. Closely associated with the XO nuclear envelope is a meshwork of primarily B-type lamin filaments (Lourim and Krohne, 1993), which are conserved in metazoan evolution and essential for mammalian cell viability (Cohen et al., 2001; Harborth et al., 2001). Lamins have central roles in nuclear architecture and nuclear integrity (Gruenbaum et al., 2003), and nuclei assembled in lamin-depleted *Xenopus* egg extracts are extremely fragile (Newport et al., 1990). Structurally, lamin filaments in the XO nucleus form a square-mesh lattice (Aebi et al., 1986) that anchors nuclear pore complexes (NPCs) (Davis, 1995; Stoffler et al., 2003). NPCs allow free diffusion of solutes and small molecules, but regulate the passage of molecules larger than 40 kDa (Suntharalingam and Wente, 2003).

In this study XO nuclear envelopes were manipulated by osmotic swelling with high molecular mass dextrans and micropipette aspiration to determine the elastic properties of the nuclear envelope, independent of the nucleoplasm. We show that given sufficient input force, the lamina network can expand uniformly to nearly twice its original surface area. Our findings provide the first quantitative measures of nuclear envelope mechanics and suggest that the native state of the XO nuclear lamina is a relatively compressed network of nearly rigid rods.

Materials and Methods

Xenopus oocyte collection and nuclear isolation

Fresh *Xenopus laevis* oocytes were obtained from sectioned ovaries (kind gifts from J. Foskett) obtained using an approved animal protocol (Jiang et al., 1998). Oocytes were separated and manually defolliculated using forceps. To obtain nuclei we dissected oocytes at the equator between the animal and vegetal hemispheres and manually teased the nucleus away from the cytoplasm into buffered isolation medium [BIM: 140 mM KCl (Fisher Scientific, Pittsburgh, PA, USA), 10 mM Hepes (Sigma-Aldrich, St Louis, MO, USA) pH 7.3 by KOH]. Various concentrations of 518 kDa dextran or 500 kDa dextran sulfate (Sigma-Aldrich) were added to BIM to control the degree of nuclear swelling during isolation. Other reagents such as sucrose, $MgCl_2$, $CaCl_2$, $NiCl_2$ and other heavy metals or divalent salts (Fisher Scientific) were included in BIM for specific experiments. Swollen nuclei were also exposed to various concentrations of Triton X-100 (Sigma-Aldrich) in BIM. Nuclei were visualized at room temperature with either a Nikon TE300 inverted microscope or Nikon SMZ1500 stereoscopic zoom microscope with a beam splitter and attached video-rate camera, JE8242 (Javelin Systems, Torrance, CA, USA).

Micropipette aspiration

Isolated nuclei were aspirated into 197 or 278 μm inner diameter glass pipettes (Drummond Scientific, Broomall, PA, USA) attached to a water-filled manometer with reservoirs of adjustable height. Pressures ranging from 1 to 40 mm water were applied with a combination of syringe suction and reservoir height adjustment via micrometer, and pressures were measured with a pressure transducer (Validyne, Northridge, CA, USA).

Fluorescent labeling of nucleoplasm, lamina and membrane

Isolated nuclei were incubated with YO-PRO, an intercalating monomeric cyanine reagent that stains double and single stranded DNA and RNA (Molecular Probes, Eugene, OR, USA). The nuclear membrane was visualized using the lipophilic dye FM4-64 (Molecular Probes). The nuclear lamina was labeled by first exposing isolated nuclei to a 0.1% solution of Triton X-100 in BIM for 30 minutes and then incubating with murine anti-lamin B2 antibody X223 (Lourim et al., 1996) followed by TRITC-conjugated anti-mouse antibody (Sigma-Aldrich). Fluorescence was visualized at room temperature on a Nikon TE300 inverted microscope with a 4× (0.13 NA) objective using a liquid nitrogen cooled CCD camera (Roper Scientific, Trenton, NJ, USA).

Data analysis

Video images were captured from standard videocassette recorder tape using Scion Image (Scion Corporation, Frederick, MD). Lengths and areas of captured digital images were measured using Scion Image.

Model of osmotic swelling as Poiseuille flow

The movement of buffer through NPCs, which caused nuclear envelope swelling, was modeled as Poiseuille flow of BIM (or water) of viscosity η through rigid pores in a continuous membrane. We assumed that diffusion of water across the two lipid bilayers was insignificant compared to flow through the pores. The number of pores per area p, the inner pore radius a (Akey, 1991) and the pore length l (Mazzanti et al., 2001) were obtained from the *Xenopus* oocyte literature. From these numbers, a filtration coefficient ϕ was determined as:

$$\phi = \frac{p\pi a^4}{8\eta l}$$

The filtration coefficient, which represents the resistance of the membrane to flow, was related to the volume flux of water J_V and the driving force. The driving force was defined as the balance between an effective osmotic pressure Π and the resisting pressure ΔP due to the membrane:

$$J_V = \phi\left(\Delta P - \Pi\right)$$

Initially, the trans-membrane ΔP was assumed to be negligible and the flux was proportional only to ϕ and Π. The osmotic pressure, which represents a solute gradient across the membrane, stayed relatively constant throughout swelling since the nucleoplasm did not expand or disperse in the entrained isolation media. When swelling reached equilibrium there was no influx (J_V is zero and ΔP is equal to Π), and the final effective membrane pressure ΔP was calculated as a function of the filtration coefficient ϕ and the initial volume influx $J_{V,\,init}$ or $(dV/dt)_{init}/SA_{init}$, where $(dV/dt)_{init}$ is the change in volume with time SA_{init} is the initial surface area. The volume influx was determined as a geometric function of the kinetic data obtained from the initial phase of swelling (see Results):

$$\Delta P = \frac{\left(dV/dt\right)_{init}}{SA_{init}\,\phi}$$

The Law of Laplace relates membrane tension to trans-membrane pressure and radius of the nucleus r.

$$T = \frac{1}{2} r \Delta P$$

The effective strain on the nuclear envelope was determined from the final area expansion α_{final}, which was defined as the area of the swollen nuclear envelope SA_{final} less the area prior to swelling SA_{init}, divided by the initial area.

$$\alpha_{final} = \frac{SA_{final} - SA_{init}}{SA_{init}}$$

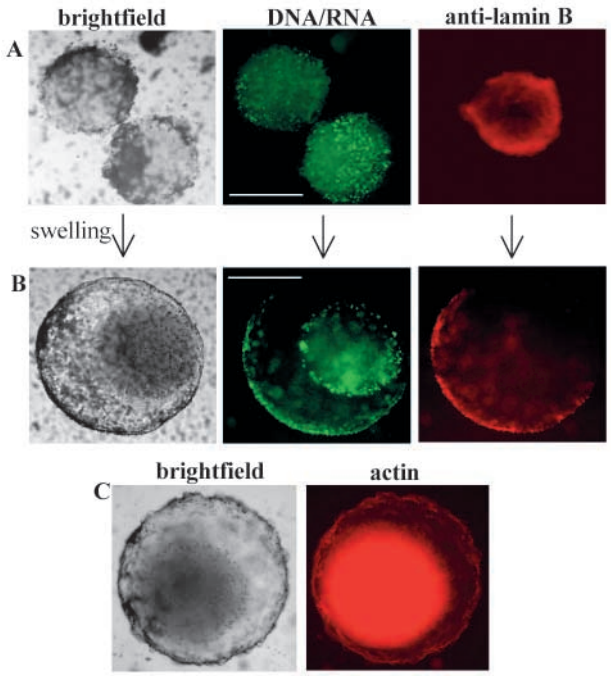

Fig. 1. Nuclear membranes and lamina detach from bulk nucleoplasm during swelling. (A) Two unswollen nuclei were imaged at 4× magnification by bright-field microscopy and stained with YO-PRO to visualize DNA/RNA in the nucleoplasm. The nucleoplasm in the unswollen nuclei completely fills the nucleus. Fluorescent antibodies against B-type lamins show the peripheral lamina of a different nucleus. (B) A single swollen nucleus was imaged by bright-field and fluorescence microscopy to reveal DNA/RNA in the nucleoplasm with YO-PRO (green) and lamins (red). The nuclear envelope, with attached lamina, detaches from the constant-size nucleoplasm during swelling. (C) A swollen nucleus imaged with bright-field optics (left) and with fluorescent phalloidin to visualize F-actin (right). Extensive actin polymerization as seen here is an artifact of nuclear isolation. Scale bars: 250 μm.

Results

Swelling separates the nuclear envelope and lamins away from the nucleoplasm

When isolated into buffered isolation medium (BIM), *Xenopus* oocyte (XO) nuclei remained spherical but swelled two-fold in diameter (Fig. 1A,B; see Materials and Methods). The nuclear lamina co-expanded with the membranes, as shown by indirect immunofluorescence staining of both unswollen and swollen nuclei (Fig. 1A,B). The apparently equal dilation at all points on the envelope was consistent with a relatively homogeneous, two-dimensional network of peripheral lamin filaments. In contrast, the nucleoplasm and chromatin did not swell, but remained the same size in both swollen and unswollen nuclei (Fig. 1A,B), probably due in part to polymerization of nuclear actin upon isolation of nuclei in BIM buffer (Fig. 1C). Polymerization of actin within XO nuclei after extraction has been reported previously (Pederson and Aebi, 2002). When visualized as either an off-center phase-dense body in bright-field microscopy, or using the fluorescent DNA/RNA dye YO-PRO, the bulk of nucleoplasmic actin and chromatin typically remained attached to one side of the swollen envelope. There was little or no evidence of envelope distortion at the attachment region, and it would appear that the site of attachment was random. A small fraction of YO-PRO-stained DNA/RNA remained associated with the swollen envelope.

Swelling was due to the entry of phase-light buffer. We concluded that the nuclear envelope remained largely intact, and buffer entered through NPCs because, as shown below, swelling was reversible by changing the extracellular solutes. Furthermore, small particles in the buffer-filled space between nuclear envelope and nucleoplasm exhibited Brownian motion very similar to particles outside the nucleus (data not shown). These buffer-filled, swollen nuclei were well suited to evaluating the mechanical properties of the nuclear envelope and its associated lamina network, largely independent of nuclear contents.

Micropipette aspiration of single nuclei

We labeled nuclear membranes with a fluorescent dye, and then aspirated the nuclear envelope, stepwise, into a micropipette (of radius R_p). This experiment demonstrated that the XO nuclear envelope was extremely deformable (Fig. 2). Small lipid vesicles and granules bound to the envelope were also labeled. When aspirated, the swollen nuclear envelope deformed in response to the applied stress. The enclosed material, mostly buffer, offered little elastic resistance. The

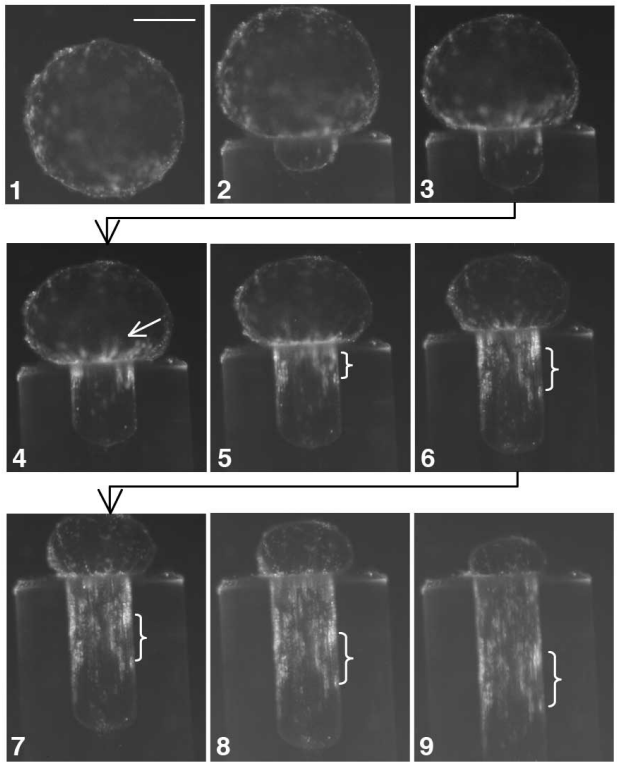

Fig. 2. Progressive aspiration of a swollen *Xenopus* oocyte nucleus. The *Xenopus* oocyte nucleus was labeled with the membrane dye FM 4-64 and progressively aspirated into a micropipette. Each image (1-9) was taken after rapid equilibration with a set imposed pressure. Note the membrane wrinkles near the pipette entrance (white arrow) consistent with shear resistance of a solid-like network. The distance between the bracketed fluorescence spots increases, thus showing local envelope stretching of nearly 300%. Scale bar: 250 μm.

nuclear membranes wrinkled near the entrance of the micropipette (Fig. 2, white arrow). For large extension lengths (L) of membrane into the micropipette ($L>R_p$, as in Fig. 2 panels 4-9), these folds indicate that the nuclear envelope and lamina behave as a solid-like network that resists membrane extension, since a fluid membrane under such pressures would smooth to relax any imposed bending strain (Discher et al., 2002). By tracking the distance between intense fluorescence spots along the projection length, the membrane is seen to stretch locally as it was being pulled into the micropipette. Some of these fluorescent markers, including the pair bracketed in Fig. 2, reveal membrane stretching up to 300% from the point at which the surface markers became visibly distinct (Fig. 2, panel 5) up to complete aspiration of the nucleus (Fig. 2, panel 9).

Determination of the network elastic modulus by micropipette aspiration

The nucleoplasm was highly deformable in unswollen nuclei (Fig. 3A). Nevertheless to test whether nucleoplasm influenced the mechanical resistance of the envelope, we aspirated swollen nuclei starting at a point distant from the nucleoplasmic body (Fig. 3A). The resistance of the envelope and its attached lamina was the same whether we aspirated at positions distal to, or near, the nucleoplasmic body. Resistance was specifically determined from the imposed pressure and resulting deformation. The pressure applied by the micropipette imposes a membrane tension on the nuclear envelope. This tension is calculated from the Law of Laplace and plotted against the dimensionless extension length (L/R_p), yielding a straight line (Fig. 3B).

The slope of the tension versus (L/R_p) line gives an extensional stiffness, E (Evans and Skalak, 1980), which can also be referred to as a network elastic modulus as discussed below. Swollen and unswollen nuclei had very similar average Es of 24 mN/m and 28 mN/m, respectively (Table 1). The statistically identical Es for swollen and unswollen nuclei

Table 1. Swollen and unswollen nuclei show similar network elastic moduli by micropipette aspiration

Nuclear state	Network elastic modulus, E
Swollen (*n*=7)	24±9 mN/m
Unswollen (*n*=4)	28±8 mN/m

Values are means±s.d.

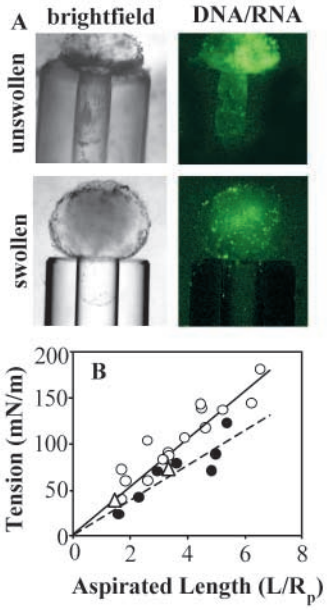

Fig. 3. Micropipette aspiration of swollen and unswollen nuclei. (A) Bright-field and DNA/RNA (labeled with YO-PRO) fluorescence images of either unswollen or swollen nuclei aspirated into a micropipette (inner radii R_p=98 μm and 139 μm, respectively). The unswollen nucleus shows deformation of the nucleoplasm coincident with the nuclear envelope. The nucleoplasm of the swollen nucleus remains external to the micropipette. (B) Representative data of Laplace tension, a function of incremental aspiration pressure, versus aspirated length of unswollen (○) and of swollen (●) nuclei yield similar slopes (see Table 1). Aspiration is reversible since decreasing the aspiration pressure (△) follows the same trend as increased pressure (○,●).

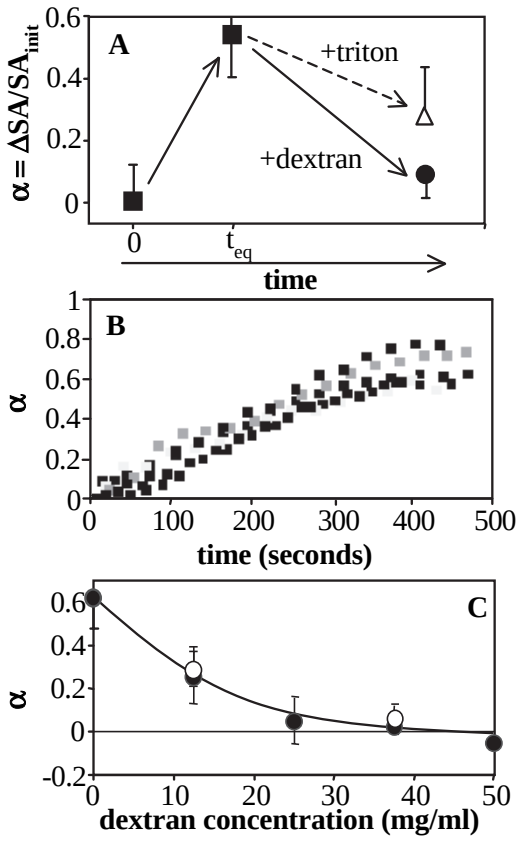

Fig. 4. Reversibility and kinetics of nuclear swelling. (A) After swelling finished in a time (t_{eq}), the relative surface area expansion (α) could be reversed with addition of dextrans (50 mg/ml). Swollen nuclei are also significantly deflated by addition of 5% Triton X-100 detergent (△) as water and solutes flow through the perforated nucleus. The nuclei remain visibly intact, nonetheless. (B) Swelling (of four nuclei) shows an initial linear increase in α with equilibration at t_{eq}=500 seconds. (C) Swelling was systematically reduced by addition of either 500 kDa dextran (●) or 500 kDa dextran sulfate (○), but concentrations of dextrans >50 mg/ml do not compress nuclei relative to their original size.

indeed demonstrate very little resistance from the nucleoplasm and suggest that XO nucleoplasm has very low intrinsic stiffness. Lastly, consistent with elastic deformation, rather than plastic or permanent deformation, aspiration of nuclear envelopes was reversible upon graded release of the pressure (triangles in Fig. 3B).

Reversible swelling of nuclei

Nuclear swelling was also reversible and, with later analysis (see the Discussion) indicative of a dilational elasticity. After swelling in BIM, nuclei were transferred into BIM containing 50 mg/ml high molecular mass (500 kDa) dextran. The dextrans returned swollen nuclei to their original unswollen size (Fig. 4A). Given that swelling was spherically symmetric (Fig. 1), relative changes in nuclear size can be reported in terms of a dimensionless increase (α) in envelope surface area (SA). Micropipette aspiration of 'de-swollen' nuclei showed that the E of the nuclear envelope lamina network was unaffected by swelling, consistent again with a highly elastic structure.

As a further control, swollen nuclei were exposed to various concentrations of the non-ionic detergent Triton X-100. With increasing Triton concentrations, nuclear surface area decreased and there was obvious weakening of the membrane. Detergent treatment perforates nuclear membranes, allowing free entry of larger solutes and buffer. In 5% Triton the nuclear envelopes became ~50% smaller as visualized by bright-field microscopy (Fig. 4A). Nuclei nonetheless maintained their spherical shape (data not shown), suggesting that the underlying lamina network remained intact. Interestingly, dextrans were more effective than Triton at restoring swollen nuclei to their original size. Dextran-induced changes in osmolarity may provide a physical driving force that restores the native state of the nuclear envelope lamina.

Rates of nuclear swelling were highly reproducible, indicative of rate-limiting fluid movement through NPCs. When swollen in BIM, nuclear surface area (α) increased at a constant rate for 300-400 seconds and reached equilibrium by 400-450 seconds (Fig. 4B). The rate and extent of nuclear swelling could be precisely controlled by varying the concentration of 500 kDa dextrans (extent shown in Fig. 4C). Visualization of fluorescently conjugated dextrans confirmed their exclusion from nuclei (data not shown), as expected from their large mass. These results confirmed that swelling was due to buffer entering the nucleus in osmotically unbalanced samples. Charge was not a factor, since swelling was blocked equally well by either neutral dextran or negatively charged dextran sulfate (Fig. 4C). In contrast, swelling was unaffected by small, neutral molecules such as sucrose, at concentrations equi-osmolar to dextrans or higher. Sucrose and similar molecules are commonly used to osmotically swell lipid vesicles (Rawicz et al., 2000). Their ineffectiveness here confirmed that swelling was due to fluid and solute transport through NPCs, not direct permeation through nuclear membranes. Divalent salts such as $MgCl_2$, $CaCl_2$ and $NiCl_2$ also had no effect on nuclear swelling (data not shown). We concluded that dextrans, excluded from the nucleus by their large mass, suppress swelling by retaining co-solutes that help to osmotically balance large osmolytes (DNA and proteins) inside the nucleus. Interestingly, nuclei were not significantly compressed even at extremely high levels of dextran (Fig. 4C).

Discussion

One obstacle to quantifying mechanical properties of the somatic nuclear envelope is its association with chromatin, which is mediated by envelope lamins themselves as well as other membrane proteins (Foisner, 2003; Gant and Wilson, 1997; Gruenbaum et al., 2003; Moir et al., 1995). Isolated chromosomes have a Young's modulus of approximately 5 kPa (Houchmandzadeh et al., 1997), which is similar to a stiff collagen gel and within the range of elasticities measured for whole nuclei in somatic cells [1-8 kPa (Caille et al., 2002; Guilak et al., 2000)]. To minimize chromatin contributions, it is possible to make nuclear envelope 'ghosts' stripped of chromatin, but their preparation involves harsh chemical and physical manipulation (Graham and Rickwood, 1997) that may compromise nuclear envelope integrity. In contrast, the XO nuclear envelope has proved, in this work, to be readily accessible to manipulation and characterization.

Micropipette aspiration of swollen and unswollen nuclei gave similar values (~25 mN/m) for the network elastic modulus, E. Thus the nucleoplasm of the XO nucleus is not stiff enough to contribute any resistance to aspiration. An easily deformable nucleoplasm is most likely unique to XO nuclei because of their extremely large size and low chromatin density. Swollen and unswollen XO nuclei appear to provide a powerful experimental system for studying the mechanics of intact nuclear envelope lamin networks.

Dilational elasticity from swelling XO nuclei

The initial kinetics of buffer flow into the nucleus during swelling (Fig. 4B) was used to estimate the elastic modulus for nuclear envelope dilation. From equations developed as a model for osmotic swelling (see Materials and Methods) we estimate that a fully swollen nucleus is under a significant tension (Fig. 5). The slope of the best fit line of tension versus α indicates an approximate dilation modulus, K, for the XO nuclear envelope of ~390 mN/m (Fig. 5). Somewhat lower area dilation moduli are seen for single bilayers of pure lipid (150-250 mN/m) (Rawicz et al., 2000). For two closely apposed

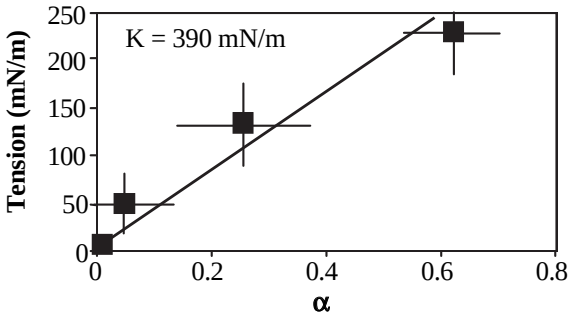

Fig. 5. Estimated nuclear envelope tension versus surface area expansion α. The tensions are calculated from kinetic swelling data and suggest that swollen nuclear envelopes are under increasing tension. The slope gives an approximate membrane dilation modulus, K.

bilayers in a multilamellar vesicle, which better approximates the two bilayers of the nucleus, the apparent membrane modulus increased relative to a unilamellar vesicle by 1.6-fold (Kwok and Evans, 1981). This gives a range of lipid moduli close to our finding here for intact nuclear envelopes.

The similar values for the membrane dilation moduli of nuclear envelopes and double bilayer lipid vesicles might suggest that membrane properties dominate nuclear envelope swelling. However, large differences in apparent lysis strain revealed properties unique to the nuclear envelope. Red cell membranes and lipid vesicles are limited in area expansion by lipid-lipid or lipid-protein interactions and lyse when the surface area increases by no more than 5% (Evans et al., 1976). In striking contrast, our results show that the nuclear membrane surface area can expand by 60%. This difference might in part result from either the ability of NPCs to dilate (Danker and Oberleithner, 2000), changes in membrane curvature at nuclear pores, smoothing of superficial membrane folds or combinations thereof.

Nuclear envelope elastic moduli

Stretching, dilating and bending of a cell membrane are generally considered independent modes of membrane deformation. With the extensional modulus E representing membrane stretching in micropipette aspiration, and with K obtained from nuclear swelling assays, it should come as no surprise that these quantities are numerically different. The structural origins of E seem relatively clear. Not only was E the same for swollen and unswollen nuclei, which thus eliminates the contributions of nucleoplasm, membrane-associated protein networks are generally known to resist deformation during micropipette aspiration (Evans and Skalak, 1980). Thus, in our experiments E measures the resistance of the lamin network to both shear and dilation, thus making E an effective two-dimensional Young's modulus for the lamin network.

Comparisons with E in other membrane systems are insightful. The red blood cell membrane is an especially well studied lipid-plus-protein-network, with a widely reported E of ~0.01 mN/m based largely on micropipette aspiration measurements (Mohandas and Evans, 1994). The nuclear lamina's E of ~25 mN/m is about three orders of magnitude stiffer. The difference is undoubtedly due to the larger stiffness of proteins in the lamin network, since protein stiffness is linearly related to the network E (Boal, 2002). Protein filament networks in both systems have a similar density, but spectrin filaments, which constitute the red cell network, are significantly softer than lamins. For filamentous proteins, persistence length is a measure of stiffness, and spectrin has a small persistence length of just 2.5-10 nm (Discher et al., 1998; Lenormand et al., 2003). Electron microscopy images of lamins suggest that they are far stiffer (Aebi et al., 1986) with persistence lengths much longer than that of spectrin. Moreover lamins are type V intermediate filament proteins, and other intermediate filament proteins have persistence lengths measured to be in the range of 100-1000 nm (Hohenadl et al., 1999).

Although highly extensible (E) and dilatable (K), the XO nucleus was also found here to have clear limits to compressibility from its native state since high concentrations of dextran in the isolation buffer did not reduce nuclear size below the native state. The chromatin seems too sparse to limit compression and had no notable influence on E. Though the nucleoplasmic actin was polymerized (phalloidin stained) as an artifact of nuclear isolation, aspiration of the nucleus into a micropipette showed that the nucleoplasm contributes little if any resistance to compression. Still, there exists a possibility that the nucleoplasm resists compression from the dextran-induced driving forces. However, we think the nuclear lamina network is more likely to limit compressibility.

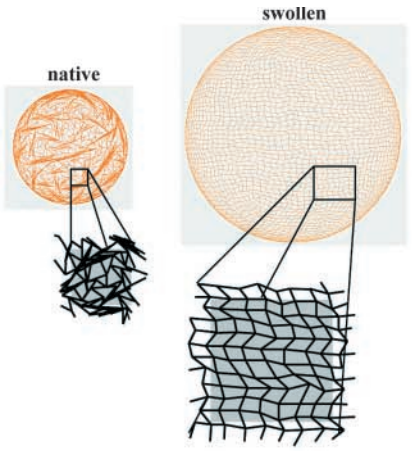

Fig. 6. Simulations of lamin rearrangement during nuclear swelling. The native nuclear lamina is in a 'compressed' state that expands to the flat, orthogonal network seen in electron micrographs of *Xenopus* oocyte lamina (Aebi et al., 1986). The compressed native state may contain domains of differing lamin interactions. Simulations are extended from those of Tessier et al. (Tessier et al., 2003).

Nuclear lamina superstructure

The present understanding of nuclear lamina organization posits a two-dimensional network of orthogonal lamin filaments (Aebi et al., 1986). How might dilation and incompressibility occur in this structure? Square mesh networks are known to collapse locally in response to two-dimensional compressive forces (Tessier et al., 2003). Figure 6 shows Monte Carlo simulations of a square mesh network on two spheres of different diameters. Both networks have the same number of 'nodes' or interconnects. Collapsed regions of the mesh are present in the smaller 'native' state of the nucleus (Fig. 6, left), but these collapsed regions expand in a fully dilated, swollen nucleus (Fig. 6, right). Interestingly, deconvolution microscopy of interphase nuclei suggests lamins are organized non-homogeneously (Paddy et al., 1990), consistent with the model of the native state proposed from this work.

While locally collapsed network domains might intrinsically oppose further compression, 'stabilizer' elements, such as nuclear actin and membrane proteins that bind actin/lamins, might also play active roles. There is growing evidence that actin has multiple roles in the nucleus (Fig. 1C) (Bettinger et al., 2004; Pederson and Aebi, 2002). Indeed, G-actin binds directly to A-type lamins (Sasseville and Langelier, 1998) and also to emerin, an integral membrane protein (Lattanzi et al.,

2003). Emerin also binds directly to F-actin, and stabilizes F-actin by capping the pointed end in vitro (Holaska et al., 2004). Other plausible stabilizer elements include the nesprin family of integral nuclear membrane proteins, some isoforms of which bind actin, lamins and emerin (Mislow et al., 2002; Zhang et al., 2002; Zhen et al., 2002). Sun-domain proteins might also act as mechanical stabilizers (Lee et al., 2002). Other structures, including an actin-dependent network of filaments that link NPCs to intranuclear organelles in XO nuclei, do not include lamins (Kiseleva et al., 2004) and are unlikely to contribute to the native compressed state of the lamina. However, we speculate that NPC-linked structures might limit the extent of envelope expansion during swelling.

With or without putative 'stabilizers', our findings support the idea of a natively compressed lamina. This collapsed network of stiff lamin rods appears to require significant energy to rearrange. Furthermore lamin filaments must be both stiff and linearly elastic over a wide range of strains in order to explain our linear aspiration results for both swollen and unswollen nuclei. Given that lamins also interact with chromatin (Gruenbaum et al., 2003), our findings have intriguing implications for the lamin-dependence of gene expression (Spann et al., 2002) if, as we propose, the lamina network acts as a 'molecular shock-absorber' with elastic extensibility but a clear limit to compressibility from the native state. Given the high conservation of B-type lamins throughout metazoan evolution (Herrmann et al., 2003), the properties of XO nuclei revealed here are likely to be widely applicable to somatic nuclei. A nearly incompressible (though dilatable) envelope would help protect chromatin and nuclear domains from compressive stresses. The proposed 'compressed' native state of the nuclear lamina network would also allow for significant strength and flexibility during shear and extension, conferring clear advantages to motile cells crawling through tissues as well as non-motile but actively deforming cells such as muscle cells. Finally, a 'compressed' native state might facilitate the transmission of mechanical force signals across the nuclear envelope.

The authors thank J. K. Foskett and G. Dreyfuss at the University of Pennsylvania and members of their laboratories, M. Ferreri-Jacobia, D. Mak, N. Petrenko and J. Yong who supplied oocytes and helpful information. The authors also thank J. Gall at the Carnegie Institute, Baltimore, MD and M. Goulian at the University of Pennsylvania for helpful conversations. This work was funded by grants from the Whitaker Foundation (K.N.D.), the Muscular Dystrophy Association (K.L.W., D.E.D.) and an NIH-BRP grant (D.E.D.).

References

Aebi, U., Cohn, J., Buhle, L. and Gerace, L. (1986). The nuclear lamina is a meshwork of intermediate-type filaments. *Nature* **323**, 560-564.

Akey, C. W. (1991). Probing the structure and function of the nuclear pore complex. *Semin. Cell Biol.* **2**, 167-177.

Bettinger, B. T., Gilbert, D. M. and Amberg, D. C. (2004). Actin in the nucleus. *Nat. Rev. Mol. Cell Biol.* **5**, 410-415.

Bissell, M. J., Weaver, V. M., Lelievre, S. A., Wang, F., Petersen, O. W. and Schmeichel, K. L. (1999). Tissue structure, nuclear organization, and gene expression in normal and malignant breast. *Cancer Res.* **59**, 1757-1763.

Boal, D. H. (2002). *Mechanics of the Cell*. Cambridge, UK: Cambridge University Press.

Burke, B. and Stewart, C. L. (2002). Life at the edge: the nuclear envelope and human disease. *Nat. Rev. Mol. Cell Biol.* **3**, 575-585.

Caille, N., Thoumine, O., Tardy, Y. and Meister, J. J. (2002). Contribution of the nucleus to the mechanical properties of endothelial cells. *J. Biomech.* **35**, 177-187.

Cohen, M., Lee, K. K., Wilson, K. L. and Gruenbaum, Y. (2001). Transcriptional repression, apoptosis, human disease and the functional evolution of the nuclear lamina. *Trends Biochem. Sci.* **26**, 41-47.

Dadoune, J. P. (2003). Expression of mammalian spermatozoal nucleoproteins. *Microsc. Res. Tech.* **61**, 56-75.

Danker, T. and Oberleithner, H. (2000). Nuclear pore function viewed with atomic force microscopy. *Pflugers Arch.* **439**, 671-681.

Davis, L. I. (1995). The nuclear pore complex. *Annu. Rev. Biochem.* **64**, 865-896.

De Sandre-Giovannoli, A., Bernard, R., Cau, P., Navarro, C., Amiel, J., Boccaccio, I., Lyonnet, S., Stewart, C. L., Munnich, A., le Merrer, M. et al. (2003). Lamin a truncation in Hutchinson-Gilford progeria. *Science* **300**, 2055.

Discher, D. E., Boal, D. H. and Boey, S. K. (1998). Simulations of the erythrocyte cytoskeleton at large deformation. II. Micropipette aspiration. *Biophys. J.* **75**, 1584-1597.

Discher, B. M., Bermudez, H., Hammer, D. A., Discher, D. E., Won, Y. Y. and Bates, F. S. (2002). Cross-linked polymersome membranes: vesicles with broadly adjustable properties. *J. Phys. Chem.* **106**, 2848-2854.

Eriksson, M., Brown, W. T., Gordon, L. B., Glynn, M. W., Singer, J., Scott, L., Erdos, M. R., Robbins, C. M., Moses, T. Y., Berglund, P. et al. (2003). Recurrent de novo point mutations in lamin A cause Hutchinson-Gilford progeria syndrome. *Nature* **423**, 293-298.

Evans, E. and Skalak, R. (1980). *Mechanics and Thermodynamics of Biomembranes*. Boca Raton, FL: CRC Press.

Evans, E. A., Waugh, R. and Melnik, L. (1976). Elastic area compressibility modulus of red cell membrane. *Biophys. J.* **16**, 585-595.

Foisner, R. (2003). Cell cycle dynamics of the nuclear envelope. *ScientificWorldJournal* **3**, 1-20.

Gant, T. M. and Wilson, K. L. (1997). Nuclear assembly. *Annu. Rev. Cell. Dev. Biol.* **13**, 669-695.

Graham, J. M. and Rickwood, D. (1997). *Subcellular fractionation: a practical approach*. Oxford, UK: Oxford University Press.

Gruenbaum, Y., Goldman, R. D., Meyuhas, R., Mills, E., Margalit, A., Fridkin, A., Dayani, Y., Prokocimer, M. and Enosh, A. (2003). The nuclear lamina and its functions in the nucleus. *Int. Rev. Cytol.* **226**, 1-62.

Guilak, F. (1995). Compression-induced changes in the shape and volume of the chondrocyte nucleus. *J. Biomech.* **28**, 1529-1541.

Guilak, F., Tedrow, J. R. and Burgkart, R. (2000). Viscoelastic properties of the cell nucleus. *Biochem. Biophys. Res. Commun.* **269**, 781-786.

Harborth, J., Elbashir, S. M., Bechert, K., Tuschl, T. and Weber, K. (2001). Identification of essential genes in cultured mammalian cells using small interfering RNAs. *J. Cell Sci.* **114**, 4557-4565.

Herrmann, H., Hesse, M., Reichenzeller, M., Aebi, U. and Magin, T. M. (2003). Functional complexity of intermediate filament cytoskeletons: from structure to assembly to gene ablation. *Int. Rev. Cytol.* **223**, 83-175.

Hoffmann, K., Dreger, C. K., Olins, A. L., Olins, D. E., Shultz, L. D., Lucke, B., Karl, H., Kaps, R., Muller, D., Vaya, A. et al. (2002). Mutations in the gene encoding the lamin B receptor produce an altered nuclear morphology in granulocytes. *Nat. Genet.* **31**, 410-414.

Hohenadl, M., Storz, T., Kirpal, H., Kroy, K. and Merkel, R. (1999). Desmin filaments studied by quasi-elastic light scattering. *Biophys. J.* **77**, 2199-2209.

Holaska, J. M., Kowalski, A. K. and Wilson, K. L. (2004). Emerin caps the pointed end of actin filaments: evidence for an actin cortical network at the nuclear inner membrane. *PloS Biol. (in press)*.

Houchmandzadeh, B., Marko, J. F., Chatenay, D. and Libchaber, A. (1997). Elasticity and structure of eukaryote chromosomes studied by micromanipulation and micropipette aspiration. *J. Cell Biol.* **139**, 1-12.

Jiang, Q., Mak, D., Devidas, S., Schwiebert, E. M., Bragin, A., Zhang, Y., Skach, W. R., Guggino, W. B., Foskett, J. K. and Engelhardt, J. F. (1998). Cystic fibrosis transmembrane conductance regulator-associated ATP release is controlled by a chloride sensor. *J. Cell Biol.* **143**, 645-657.

Kiseleva, E., Drummond, S. P., Goldberg, M. W., Rutherford, S. A., Allen, T. D. and Wilson, K. L. (2004). Actin- and protein-4.1-containing filaments link nuclear pore complexes to subnuclear organelles in Xenopus oocyte nuclei. *J. Cell Sci.* **117**, 2481-2490.

Kwok, R. and Evans, E. (1981). Thermoelasticity of large lecithin bilayer vesicles. *Biophys. J.* **35**, 637-652.

Lattanzi, G., Cenni, V., Marmiroli, S., Capanni, C., Mattioli, E., Merlini,

L., Squarzoni, S. and Maraldi, N. M. (2003). Association of emerin with nuclear and cytoplasmic actin is regulated in differentiating myoblasts. *Biochem. Biophys. Res. Commun.* **303**, 764-770.

Lee, K. K., Starr, D., Cohen, M., Liu, J., Han, M., Wilson, K. L. and Gruenbaum, Y. (2002). Lamin-dependent localization of UNC-84, a protein required for nuclear migration in Caenorhabditis elegans. *Mol. Biol. Cell* **13**, 892-901.

Lenormand, G., Henon, S., Richert, A., Simeon, J. and Gallet, F. (2003). Elasticity of the human red blood cell skeleton. *Biorheology* **40**, 247-251.

Lourim, D., Kempf, A. and Krohne, G. (1996). Characterization and quantitation of three B-type lamins in Xenopus oocytes and eggs: increase of lamin LI protein synthesis during meiotic maturation. *J. Cell Sci.* **109**, 1775-1785.

Lourim, D. and Krohne, G. (1993). Membrane-associated lamins in Xenopus egg extracts: identification of two vesicle populations. *J. Cell Biol.* **123**, 501-512.

Maniotis, A. J., Chen, C. S. and Ingber, D. E. (1997). Demonstration of mechanical connections between integrins, cytoskeletal filaments, and nucleoplasm that stabilize nuclear structure. *Proc. Natl. Acad. Sci. USA* **94**, 849-854.

Mazzanti, M., Bustamante, J. O. and Oberleithner, H. (2001). Electrical dimension of the nuclear envelope. *Physiol. Rev.* **81**, 1-19.

Mislow, J. M., Holaska, J. M., Kim, M. S., Lee, K. K., Segura-Totten, M., Wilson, K. L. and McNally, E. M. (2002). Nesprin-1alpha self-associates and binds directly to emerin and lamin A in vitro. *FEBS Lett.* **525**, 135-140.

Mohandas, N. and Evans, E. (1994). Mechanical properties of the red cell membrane in relation to molecular structure and genetic defects. *Annu. Rev. Biophys. Biomol. Struct.* **23**, 787-818.

Moir, R. D., Spann, T. P. and Goldman, R. D. (1995). The dynamic properties and possible functions of nuclear lamins. *Int. Rev. Cytol.* **162**, 141-182.

Morris, G. E. (2001). The role of the nuclear envelope in Emery-Dreifuss muscular dystrophy. *Trends Mol. Med.* **7**, 572-577.

Newport, J. W., Wilson, K. L. and Dunphy, W. G. (1990). A lamin-independent pathway for nuclear envelope assembly. *J. Cell Biol.* **111**, 2247-2259.

Paddy, M. R., Belmont, A. S., Saumweber, H., Agard, D. A. and Sedat, J. W. (1990). Interphase nuclear envelope lamins form a discontinuous network that interacts with only a fraction of the chromatin in the nuclear periphery. *Cell* **62**, 89-106.

Papadaki, M. and Eskin, S. G. (1997). Effects of fluid shear stress on gene regulation of vascular cells. *Biotechnol. Prog.* **13**, 209-221.

Pederson, T. and Aebi, U. (2002). Actin in the nucleus: what form and what for? *J. Struct. Biol.* **140**, 3-9.

Rawicz, W., Olbrich, K. C., McIntosh, T., Needham, D. and Evans, E. (2000). Effect of chain length and unsaturation on elasticity of lipid bilayers. *Biophys. J.* **79**, 328-339.

Sasseville, A. M. and Langelier, Y. (1998). In vitro interaction of the carboxy-terminal domain of lamin A with actin. *FEBS Lett.* **425**, 485-489.

Spann, T. P., Goldman, A. E., Wang, C., Huang, S. and Goldman, R. D. (2002). Alteration of nuclear lamin organization inhibits RNA polymerase II-dependent transcription. *J. Cell Biol.* **156**, 603-608.

Stoffler, D., Feja, B., Fahrenkrog, B., Walz, J., Typke, D. and Aebi, U. (2003). Cryo-electron tomography provides novel insights into nuclear pore architecture: implications for nucleocytoplasmic transport. *J. Mol. Biol.* **328**, 119-130.

Suntharalingam, M. and Wente, S. R. (2003). Peering through the pore: nuclear pore complex structure, assembly, and function. *Dev. Cell* **4**, 775-789.

Tessier, F., Boal, D. H. and Discher, D. E. (2003). Networks with fourfold connectivity in two dimensions. *Phys. Rev. E. Stat. Nonlin. Soft Matter Phys.* **67**, 011903.

Wilson, K. L. (2000). The nuclear envelope, muscular dystrophy and gene expression. *Trends Cell Biol.* **10**, 125-129.

Yabuki, M., Miyake, T., Doi, Y., Fujiwara, T., Hamazaki, K., Yoshioka, T., Horton, A. A. and Utsumi, K. (1999). Role of nuclear lamins in nuclear segmentation of human neutrophils. *Physiol. Chem. Phys. Med. NMR* **31**, 77-84.

Zastrow, M. S., Vlcek, S. and Wilson, K. L. (2004). Proteins that bind A-type lamins: integrating isolated clues. *J. Cell Sci.* **117**, 979-987.

Zhang, Q., Ragnauth, C., Greener, M. J., Shanahan, C. M. and Roberts, R. G. (2002). The nesprins are giant actin-binding proteins, orthologous to Drosophila melanogaster muscle protein MSP-300. *Genomics* **80**, 473-481.

Zhen, Y. Y., Libotte, T., Munck, M., Noegel, A. A. and Korenbaum, E. (2002). NUANCE, a giant protein connecting the nucleus and actin cytoskeleton. *J. Cell Sci.* **115**, 3207-3222.